Int. J. Electrochem. Sci., 16 **(2021)** Article ID: 210930, doi: 10.20964/2021.09.41

International Journal of
ELECTROCHEMICAL
SCIENCE
www.electrochemsci.org

Formic Acid Formation from the Electrochemical Reduction of Carbon Dioxide Catalyzed by a Rhodium Protoporphyrin in aqueous solution

Jing Shen[*], *Kunxiang Deng, Xiangjun Li, Donghui Lan*[*], *Zhengjun Fang*

Hunan Provincial Key Laboratory of Environmental Catalysis & Waste Recycling, School of Material and Chemical Engineering, Hunan Institute of Engineering, Xiangtan, 411104, P.R. China.
[*]E-mail: jingshen84@sina.com, donghuilan@hnu.edu.cn

Received: 28 May 2021 / *Accepted:* 13 July 2021 / *Published:* 10 August 2021

The electrochemical conversion of CO_2 into valuable fuels is a promising technique to store intermittent energy, such as wind, solar and nuclear, and facilitate a closed carbon cycle. Here we report the formation of formic acid from the electrochemical reduction of CO_2 catalyzed by rhodium-protoporphyrin in aqueous solution. The formation of formic acid is highly dependent on pH with the highest faradaic efficiency of 50% at pH=3 while it is negligible at pH=1. The theoretical predication indicates that CO should be the main product from the electrochemical reduction of CO_2 catalyzed by rhodium-protoporphyrin as cobalt-protoporphyrin. However, the strong affinity of axial ligands hinders the formation of metal-bonded carboxylate or metal-hydride intermediates leading to the difficulty of the formation of CO or formic acid through the intermediate respectively. The most likely intermediate for the formation of formic acid catalyzed by rhodium-protoporphyrin is phlorin-hydride which is an intermediate protonated the meso carbon of the macrocycle.

Keywords: rhodium-protoporphyrin; CO_2 electrochemical reduction; formic acid; phlorin-hydride

1. INTRODUCTION

Carbon dioxide released from the combustion of fossil fuels is converted into chemical energy by photosynthesis process, which accomplishes a carbon cycle in nature. However, the large discrepancy between the rate of carbon dioxide emission and plant fixation results in accumulation of carbon dioxide in the atmosphere. As well known, carbon dioxide is a notorious “green-house” gas. The increasing of carbon dioxide concentration in the atmosphere resulted from excessively combustion of fossil energy will not only lead to serious environmental problems, but also cause potential fossil energy crisis. Therefore, researchers desire to find a way to reduce the carbon dioxide emission or utilize it. [1-4]

Ideally, they want to convert carbon dioxide into valuable chemicals, such as carbon monoxide, formic acid (formate), formaldehyde, methanol and methane. [5-7] This technique can reduce the concentration of inert carbon dioxide in atmosphere and produce fuels at meanwhile. If the energy needed for the carbon dioxide conversion comes from renewable resources, such as solar, wind and nuclear, it can accomplish a carbon neutral cycle, which will greatly reduce the carbon dioxide emission. Different kinds of techniques have been utilized to facilitate carbon dioxide conversion, including chemical, [8-10] electrocatalytic and photocatalytic reduction. [11-14] The benefits of developing the electrocatalytic reduction of carbon dioxide technique are as the following: (1) the process is easily controlled by electrode potential, pressure and temperature; (2) water can be used as the hydrogen source; (3) the electrolyte can be fully recycled; (4) the electricity for driving the process can be produced from renewable energy, therefore the generating of new carbon dioxide could be avoided. [15] However, there still are certain barriers hindering the practical application of CO_2 conversion technique, including (1) the formation of the key intermediate, $CO_2^{-}\cdot$ radical requires high energy input; (2) the competition of the hydrogen evolution reaction (HER). [16]

Molecular catalysts have been frequently used as catalyst for the electrochemical reduction of CO_2 for decades because they are relatively less expensive and more abundant comparing to noble metal catalysts. The electrochemical reduction of CO_2 is a proton assisted multi-electron transferred process. Therefore, catalysts used for catalyzing the reaction are needed to be capable of mediating the microscopic steps involve. The metal center within molecular catalyst has a variable oxidations states (including ligand), which is well appropriate for above-mentioned task and often offer tunable catalytic activity and selectivity. Furthermore, structures of molecular catalysts can be accurately modified for improving catalytic activities and investigating catalytic mechanisms. Currently a variety of molecular catalysts have been investigated as effective catalysts for the electrochemical reduction of CO_2, such as polypyridine, phosphine, cyclam, porphyrin, phthalocyanine, and other macrocyclic structures. [17-21] In addition, most of molecular catalysts used for CO_2 electrochemical reduction are conducted in homogeneous conditions, where molecular catalysts are dissolved in solution. As the solubility of most molecular catalysts is quite low in aqueous solution, the electrochemical reduction of CO_2 is normally explored in aprotic solvent. The immobilization of molecular catalyst on electrode will not only avoid the problems of dissolving molecular catalysts, but also accomplish heterogeneous catalysis. Herein, we report a rhodium-protoporphyrin immobilized pyrolytic graphite electrode as a working electrode catalyzes the electrochemical reduction of CO_2 in aqueous solution. The main product found from the process is formic acid which is different from the situation where cobalt-protoporphyrin was used as the catalyst at the same condition in our previous work indicating the different mechanism on these two similar molecules. [22]

2. MATERIAL AND METHODS

2.1. Fabrication of Working Electrode

All electrochemical experiments were conducted in a one compartment cell, except for faradaic efficiency experiments, including a platinum flag as counter electrode, a reversible hydrogen electrode

(RHE) as a reference, to which all potentials were referred in this paper, and a rhodium-protoporphyrin immobilized pyrolytic graphite electrode as working electrode. The faradic efficiency experiments have been conducted in an H-cell separated by a Nafion-film into consisted with two compartments, one of which is filled in with a working electrode and an Ag/AgCl reference electrode while the other is is with an Pt coil as a counter. All glassware was boiled in concentrated sulfuric and nitric acid (3:1) first and boiled 5 times in Milli-Q water (Milli-Q gradient A10 system, 18.2 MΩ cm) latter. The working electrode was prepared as in our previous work: [23] a cylinder pyrolytic graphite electrode with diameter of 5 mm was abraded with P500 and P1000 SiC sandpaper and ultrasonicated in Milli-Q water for 1 min. After rinsed with water and dried in compressed air, the electrode was dipped in 0.5 mM rhodium-protoporphyrin solution for 5 min. 0.2 M perchlorate electrolyte solution was prepared using $NaClO_4$ (Sigma-Aldrich, ≥ 98.0%) and $HClO_4$ (Merck, 70%). Argon was purged through electrolyte solution for 20 min before every experiment to move dissolved oxygen.

2.2. OLEMS measurements

The gaseous products were monitored using the on-line electrochemical mass spectroscopy (OLEMS) combined with cyclic voltammetry (CV) as in previous work. [24] A hydrophobic porous Teflon cylinder tip with diameter of 0.51 mm positioned closely (~ 10μm) to the center of the surface of the working electrode. The gaseous products produced were sucked into highly vacuumed (less than 10^{-6} mbar) mass spectrometer chamber through a PEEK capillary. The SEM voltages applied on all signals are 2400 V, except for hydrogen (m/z=2) which is 1200 V. The Teflon tip was cleaned prior experiments by dipping into 0.2 M $K_2Cr_2O_7$ in 2 M H_2SO_4 solution for 15 min and rinsed thoroughly with Milli-Q water. The cyclic voltammetry is conducted from 0 V to -1.5 V with a scan rate of 1 mV/s by an Ivium A06075 potentiostat.

2.3. HPLC measurements

High-performance liquid chromatography (HPLC) was combined with the linear voltammetry (LV) to detect liquid products.[25] A porous Teflon tip inner diameter of 0.38 mm was positioned closely (~ 10 μm) to the center of the working electrode. Samples with a volume of 60 μL were collected into a 96-well microtiter plate (270 μL per well, Screening Device b.v.) using an automatic fraction collector (FRC-10A, Schimadzu), while a linear voltammogram is scanned from 0 V to -1.5 V vs RHE a rate of 1 mV/s. The microtiter plate after finishing collecting samples was put onto an auto-sampler (SIL-20A) holder. A sample with a volume of 30 μL was then injected into an Aminex HPX 87-H (Bio-Rad) column of which the temperature was kept at 85 ^{0}C using a column oven (CTO-20A). A refractive index detector (RID-10A) was using to analyze samples.The eluent was diluted sulfuric acid (5 mM) with a flow rate of 0.6 mL/min. The Faradaic efficiencies of liquid products were also measured using HPLC. The electrolysis was conducted for 2h, after which 2 mL sample collected from working electrode compartment was analyzed by HPLC.

3. RESULTS AND DISCUSSION

3.1. Immobilization of Rhodium-protoporphyrin

Figure 1 shows the electrochemical response of rhodium-protoporphyrin after immobilized on pyrolytic graphite via dip-coated method at pH=1 comparing to blank pyrolytic graphite electrode. The cyclic voltammogram of blank pyrolytic graphite shows a redox peak around 0.67 V, which is related to the redox transition of quinone/hydroquinone according to the structure of pyrolytic graphite. After the immobilization of rhodium-protoporphyrin, the voltammogram exhibits an extra redox peak around 0.36 V which is ascribed to the redox transformation of Rh^{III} changed to Rh^{II}. Yamazaki and coworkers have immobilized rhodium octaethylporphyrin [Rh^{III}-(OEP)Cl] on carbon black and investigated the electrochemical properties of the system.[26] The clear Gaussian shape of the cyclic voltammograms of carbon black supported [Rh^{III}-(OEP)Cl] in 0.1 M H_2SO_4 solution suggest that the wave is derived from a molecule strongly adsorbed on carbon black. The voltammograms of rhodium protoporphyrin immobilized pyrolytic graphite as shown in Figure 1 have also exhibited a Gaussian shape indicating the successful immobilization of the molecules. The width of the peak at half-height for carbon black supported [Rh^{III}-(OEP)Cl] (95 mV for cathodic peak and 82 mV for anodic peak) indicates that there is only one electron involved in the reaction path. Therefore, the cathodic reaction has been ascribed to the following reaction:

$$[Rh^{III}(OEP)^{+}] + e^{-} \rightarrow [Rh^{II}(OEP)]$$

From Figure 1, it is clear that the width of the peak at half-height is also indicating an electron transfer process, which is as following:

$$[Rh^{III}(PP)^{+} + e^{-} + [Rh^{II}(PP)]$$

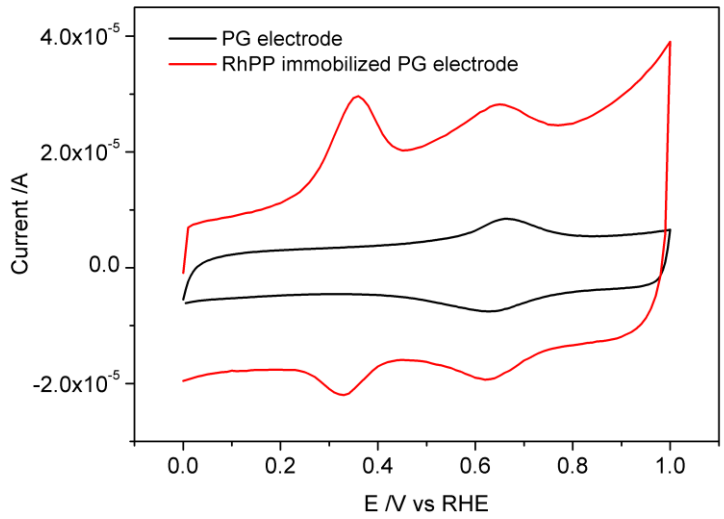

Figure 1. Cyclic voltammograms of pyrolytic graphite electrode (—), with adsorbed rhodium protoporphyrin (—), Voltammograms were measured in 0.2 M perchloric acid, pH=1.0, at a scan rate of 500 mV s^{-1}.

3.2. Catalytical activity of rhodium-protoporphyrin

The catalytic capability of rhodium protoporphyrin toward the electrochemical reduction has first been investigated using HPLC. The concentration profile of the liquid products produced from the electrochemical reduction of CO_2 on rhodium-protoporphyrin immobilized pyrolytic graphite electrode at different pH (pH=1 to pH=3) are illustrated in Figure 2. The only liquid products detected in this process is formic acid. From Figure 2 it also can be observed that the selectivity of the formic acid is highly dependent on pH. The formic acid could only be detected at pH=3 with the highest concentration of 0.19 mM. With the pH decreasing a little bit, such as to pH=2 or pH=1, the formation of formic acid has been greatly inhibited. This is probably due to the competition of the hydrogen evolution reaction (HER) as the formation of hydrogen will be dominant when the solution becomes more acidic. As discussed in our previous work, [22] the hydrogen evolution reaction which is related to direct proton (H^+) reduction will run into diffusion limitation quite fast and the water reduction will be happened at much more negative potential which is around -1.1 V. From HPLC results, the onset potential for the electrochemical reduction of CO_2 catalyzed by rhodium-protoporphyrin is around -1.2 V which is close to the onset potential of water reduction. Compared the electrochemical reduction of CO_2 to water, it can be deduced that the hydrogen source needed for the electrochemical reduction of CO_2 does not have to be proton, it would be also be other hydrogen sources instead, such as water in current process. In a word, rhodium-protoporphyrin is catalytically active for the electrochemical reduction of CO_2 to produce formic acid, and the formic acid formation prefers a little bit higher pH (pH=3) due to the competition of the hydrogen evolution reaction at lower pH and the and that the effective hydrogen source in the process can be the hydrogen in water.

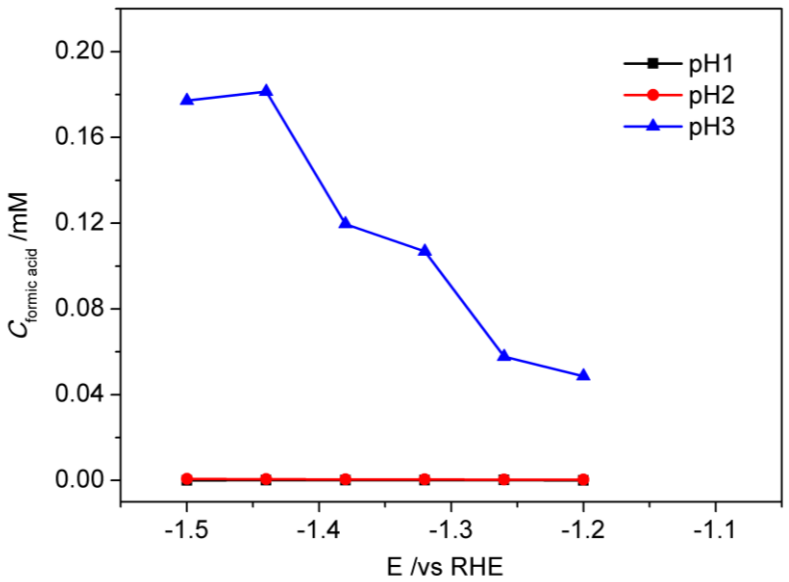

Figure 2. Plot showing the concentration of formic acid formation as a function of potential on rhodium-photoporphyrins immobilized pyrolytic graphite electrode at pH=1 (■), 2 (⬬) and 3 (▲).

3.3. Faradaic efficiency of formic acid

As the catalytical activity has been confirmed as above, it is reasonable to investigate the faradaic efficiencies of formic acid from the CO_2 electrolysis on rhodium protoporphyrin at different potentials at pH=3, which were illustrated in Figure 3 with error bars. The electrolysis has been conducted at each certain potential for 2h. And the faradaic efficiency has been calculated as following:

$$\mathrm{FE} = \frac{c_{HCOOH} \times V \times F}{I_{average} \times \Delta t}$$

Where c_{HCOOH} is the concentration of formic acid detected using HPLC, V is the volume of electrolyte used during the electrolysis, F is the faradaic constant, $I_{average}$ is the average current during the electrolysis for a certain time and Δt is the interval of the time for collecting samples. In accordance with results from HPLC, formic acid can be only produced at relatively negative potential which is more negative than -1.1 V. As the potential becoming more negative, the faradaic efficiency of formic acid is increased, reaching its maximum value of 50% at -1.2 V. As the potential applied more negative than -1.2 V, the faradaic efficiency decreases to 26%. When the electrolysis potential is -1.4 V, the faradaic efficiency of formic acid is less than 10%. The decreasing is probably owing to the competition of the hydrogen evolution reaction at such negative potential as mentioned above. It is can be found that the faradaic efficiency often exhibits big error bar. This is probably due to the sluggish diffusion of formic acid leading to the concentration gradient from electrode surface to the position where we collect samples. Besides, the samples were collected at different time, so the position for collecting samples is impossible to be controlled exactly the same at every time. In order to diminish the deviation, it is needed to stir the electrolyte during the whole electrolysis process, which is not conducted in this paper.

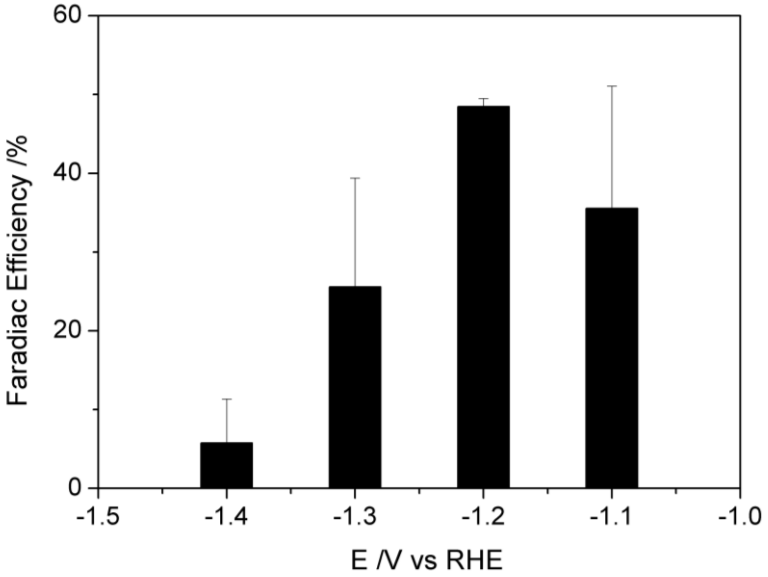

Figure 3. Faradiac efficiency of formic acid from CO_2 reduction on rhodium protoporphyrin immobilized pyrolytic graphite to formic acid at different potentials in 0.1 M perchlorate solution saturated with CO_2 at pH=3. At each potential, the electrolysis was conducted for 2h at P_{CO2}=1atm. Error bars were determined from 3-5 data points.

3.4. Volatile products formation

The formation of volatile products from CO_2 reduction catalyzed by rhodium-protoporphyrin are detected using OLEMS at pH=1 and pH=3 as shown in Figure 4. Same experiments have also been conducted at pH=2, which has the similar final results as those at pH=1 except for the lower ion current for the fragment monitored. Therefore, the results are not shown here. From Figure 4, it can be seen that only volatile product could be measured is hydrogen (m/z=2) no matter at pH=1 or pH=3. The formation of hydrogen initiated at around -0.4 V at pH=1, which is at the range of the direct proton reduction as elucidated in our previous work.[22] As pH increased to 3, the onset potential for the hydrogen formation is much more negative than that at pH=1, which is about -1.2 V. As discussed in the literature,[27] the hydrogen formation at this potential is related to the water reduction. On the other hand, this potential is right in the range where formic acid formed as elucidated as above, further confirmed above mentioned deduction that the hydrogen source for the electrochemical reduction of CO_2 is probably from water rather than protons. However, if we zoom in the potential range from -0.4 V to -1.0 V, it still can be found that the tiny amount of hydrogen is formed which runs into diffusion limitation quiet soon. As elaborated in literature,[22] the hydrogen evolution reaction occurred in this area is probably related to the direct proton reduction, whose reaction rate is proportional to the concentration of proton. Based on the HPLC and OLEMS measurements, the possible products produce from the electrochemical reduction of CO_2 catalyzed by rhodium-protoporphyrin could only be formic acid, and it is hardly reduced further to form more than 2-electron transferred products such as methanol or methane.

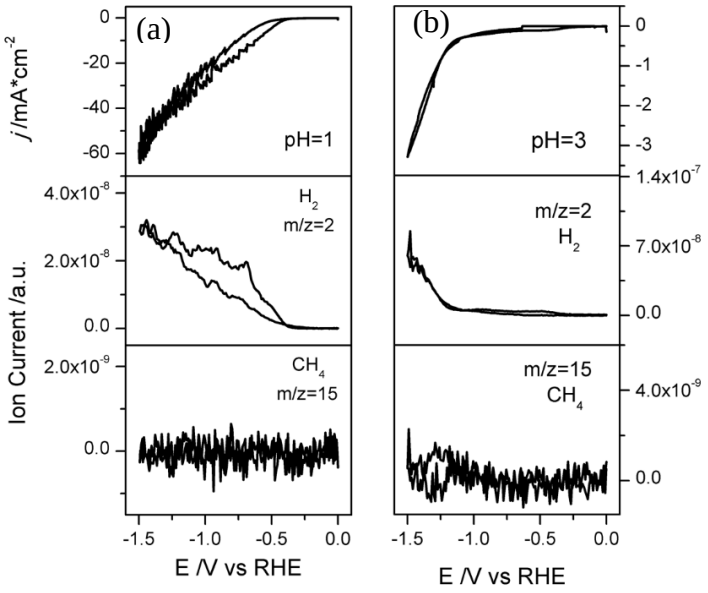

Figure 4. 4 Identification of volatile product by OLEMS with cyclic voltammagram during electrochemical reduction of CO_2 at (a) pH=1 (100 mM $HClO_4$ + 100 mM $NaClO_4$) and (b) pH=3 (1mM $HClO_4$ + 199 mM $NaClO_4$) in 0.2 M $\mathbf{ClO_4^-}$ solution saturated with CO_2. The OLEMS signals of m/z=2 and 15 corresponding to H_2 and CH_4 respectively. Scan rate: 1 mV/s.

3.5.CO and formic acid electrochemical reduction

In order to understand the mechanism of the electrochemical reduction of CO_2 catalyzed by rhodium-protoporphyrin, especially the process after the formation of 2-electron transferred products, such as methanol and methane, the electrochemical reduction of CO and formic acid catalyzed by rhodium-protoporphyrin has been investigated using HPLC and OLEMS as shown in Figure 5. No matter for the electrochemical reduction of CO or formic acid, the HPLC detection at different pH (from pH=1 to pH=3) exhibited no formation of detectable liquid products. Therefore, the concentration profiles of the liquid products from the CO and formic acid reduction have not been presented here. For the electrochemical reduction of formic acid, the only gaseous product detected is hydrogen. The OLEMS measurements related to the formic acid electrochemical reduction were not shown here neither. From Figure 5, the most obvious difference with the electrochemical reduction of CO compared to CO_2 reduction is that the onset potential of the hydrogen evolution reaction at pH=1 (-0.6 V) is a little bit more negative than the situation when the electrolyte saturated with CO_2. On the other hand, tiny amount of CH_4 (fragment m/z=15) could be detected at pH=1from the electrochemical reduction of CO. At pH=3, the onset potential for the hydrogen evolution reaction is also more negative (-1.25 V) than that with CO_2 saturated. With pH increased from 1 to 3, the formation of CH_4 is clearly suppressed with only very tiny amount at quite negative potential. Consistent with our previous discussion, the formation of CH_4 is an electron-proton concerted process which needs electron and proton transferred at the same time. Therefore, the formation of CH_4 preferred to be produced at more acidic condition such as pH=1. However, the amount of CH_4 produced from the electrochemical reduction of CO catalyzed by rhodium-protoporphyrin is quite rare, so it is impossible to quantitatively calculate the faradaic efficiency. Abdinejad and coworkers studied the electrocatalytic reduction of CO_2 to CH_4 and CO in aqueous solution using iron pyridine-porphyrins immobilized onto carbon nanotubes. [28] The greatest FE_{CH_4} achieved 41% and the highest total FE_{total} is 92% at -0.6 V vs. RHE. They also demonstrated that the heterogeneous immobilization of porphyrins on the carbon support matrix exhibited exceptional catalytic activity and selectivity, which is probably due to the rapid electron transfer between the catalyst and electrode. The proposed mechanism for the formation of CO is similar to what have published in literatures. [29] However, the process of CH_4 formation involves a multitude of electron and proton transfer steps as well as multiple reaction intermediates, leading to the complexity of providing detailed mechanism. [30]

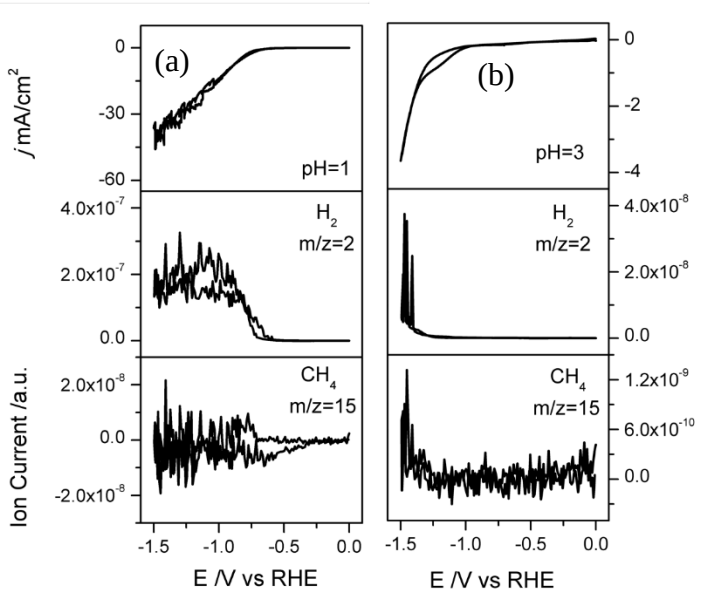

Figure 5. Identification of volatile product by OLEMS during the electrochemical reduction of CO at different pH. CV of CO reduction in in 0.2 M $\mathbf{ClO_4^-}$ with saturated CO associate mass fragments of volatile products detected with OLEMS on (a) pH=1 (100 mM $HClO_4$ + 100 mM $NaClO_4$) and (b) pH=3 (1mM $HClO_4$ + 199 mM $NaClO_4$). The OLEMS signals of m/z=2 and 15 corresponding to H_2 and CH_4 respectively. Scan rate: 1 mV/s.

From literatures, it is clear that the catalytic activity and selectivity of metal-protoporphyrins towards the electrochemical reduction of CO_2 is highly dependent on the metal center.[31-33] Birdja and Göttle et al have discussed the influence of the metal center of metalloprotoporphyrins on the electrocatalytic CO_2 reduction experimentally and theoretically.[34,35] Birdja and coworkeds explained that rhodium-protoporphyrin is the active for both hydrogen evolution reaction and CO_2 reduction leading to the relatively low faradaic efficiency. Göttle et al elucidated that the distinction between metal-electroactive and ligand-electroactive metal-porphyrin is a helpful descriptor to distinct the selectivity and the reaction pathways of the electrochemical reduction catalyzed by metal-porphyrins. The metal-electroactive metal-porphyrins included the metal centers of Fe, Co and Rh, while ligand-electroactive which is ascribed as phlorin metal-porphyrins encompass Ni, Cu, Zn, Pd, Ag, Cd, Cd, Ga, In, and Sn metal centers. The theoretical prediction indicated that the formation fo metal-bonded carboxylate and metal-hydride intermediates are much more favorable than ligand-electroactive intermediates during the process. Two reduction steps are related to Fe(III) center leading to formation of the formal Fe(0) oxidation state is necessary to trigger the electrochemical reduction of CO_2 to CO.[36] Regarding with cobalt-protoporphyrin, the metal-bonded carboxylate group is considered as the most possible intermediate for the CO or CH_4 formation following a proton-coupled electron transfer step.[37] The onset potential of CO_2 reduction on cobalt protoporphyrin appears to be related to the Co^{II}/Co^{I} redox transition. The metal-bonded carboxylate intermediate formed through a hybrid orbital consisted of cobalt metallic orbital (d_z^2 (ca. 20%) and $d_{x^2-y^2}$(ca.40%) with the antibonding $\boldsymbol{\pi}^*$ orbital (ca. 40%) of CO_2. [38] For the rhodium-protoporphyrin, the theoretical prediction is that a reduced metal center followed with the formation of a metal-bonded carboxylate intermediate leading to CO formation from

the electrochemical reduction of CO_2. However, in contrast with the theoretical prediction, CO has not been observed instead of the formic acid is found to be the only product from the electrochemical reduction of CO_2 as shown above. A strong affinity of axial ligation for rhodium catalyst has been observed experimentally. [39] The presence of axial ligands has been proved to shift the reduction potential significantly to more negative direction. Pentacoordinated hydroxo complex [Rh(III)P(OH)] exhibits the reduction potential at E ≈ -0.8 V vs RHE. The formation of formic acid or formate through the intermolecular hydride (metal hydride or the phlorin ligand) is considered to be the most possible pathway for all metal centers. The onset potential for the electrochemical reduction of CO_2 which is -1.2 V as presented above is substantially more negative than the equilibrium potential of formic acid/format formation as calculated. The formation potential of phlorin is impacted little with the possible presence of axial ligands compared to the reduction potential of rhodium center. On the other hand, the axial ligands can also hinder the formation of the metal-hydride which is the other possible intermediate for the formic acid/formate formation. In a word, the production of formic acid from the electrochemical reduction of CO_2 catalyzed by rhodium-protoporphyrin is likely to mostly proceed via the phlorin intermediate. The discrepancy between the experimental and theoretical results is due to the strong affinity of axial ligands on rhodium center.

4. CONCLUSION

Stated thus, rhodium-protoporphyrin is catalytically active for the electrochemical reduction of CO_2 with formic acid as the only product at pH=3. In more acidic electrolyte, the hydrogen evolution reaction will be dominate leading to the electrochemical reduction of CO_2 is negligible. The theoretical prediction indicates that the most favorable pathway of the electrochemical reduction of CO_2 catalyzed by rhodium-protoporphyrin should be the formation of a metal-bonded carboxylate intermediate which will finally lead to the formation of CO. However, the experimental results presented here exhibited the formation of formic acid which needs a hydride to trigger the reaction through intermolecular hydride transfer mechanism. The reason for the discrepancy is probably due to the strong affinity of axial ligation for the rhodium metal center which resulted in the difficulty of the formation of metal-active intermediate such as metal-carboxylate group or metal-hydride. Thus, the formation of formic acid is probably through phlorin intermediate. However, there is still lack of experimental evidences to confirm the hypothesis which needed further investigations.

ACKNOWLEDGEMENTS
This work was supported by the Natural Science Foundation of China (No.21703060), the Normal project of Hunan Education Department (No. 17C0391) and Hunan Province Key Laboratory of Environmental Catalysis and Waste Rechemistry (Hunan Institute of Engineering) (No. 2018KF04).

References

1. S. Bachu, Prog. *Energy. and Combust Sci.*, 34(2008) 254-273.
2. S.I. Plasynski, J.T. Litynski and R.D. Srivastava, *Crit. Rev. in Plant Sci.*, 28(2009) 123-138.

3. N.L. Panwar, S.C. Kaushik and S. Kothari, *Renew. Sust. Energy Rev.*, 15(2011) 1513-1524.
4. H. Lund, *Energy*, 32(2007) 912-919.
5. G.P.S.Lau, M. Schreier and M. Grätzel, *J. Am. Chem. Soc.*, 138(2016) 7820-7823.
6. Y.Y. Birdja, J. Shen and M.T.M. Koper, *Catalysis Today*, 288(2017) 37-47.
7. Z. Weng, J.B. Jiang and H.L. Wang, *J. Am. Chem. Soc.*, 138(2016) 8076-8079.
8. T.J. Meyer, *Coord. Chem. Rev*., 153(1996) 257-284.
9. M. Cheng, E.B. Lobkovsky and G.W. Coates, *J. Am. Chem. Soc.*, 120(1998) 11018-11019.
10. J. Omae, Coordi. Chem. Rev., 256(2012) 1384-1405.
11. T. Sakakura, J.C. Choi and H. Yasuda, *Chem. Rev.*, 107(2017) 2365-2387.
12. C. Oloman and H. Li, *ChemSusChem.*, 1(2008) 385-391.
13. C. Finn, S. Schnittger and J.B. Love, *Chem. Commun.*, 48(2012) 1392-1399.
14. K. Mor, H. Yamashita and M. Anpo, *Rsc. Adv.*, 2(2012) 3165-3172.
15. A.S. Agarwal, Y.M. Zhai and N. Sridhar, *ChemSusChem.*, 4(2011) 1301-1310.
16. G.O. Larrazábal, A.J. Martín, S. Mitchell, R. Hauert and J. Pérez-Ramírez, *ACS Catal.,* 6(2016) 6265-6274.
17. E.E. Benson, C.P. Kubiak and J.M. Smieja, *Chem. Soc. Rev.*, 38 (2009) 89-99.
18. J.L.Inglis, B.J. MacLean, M.T. Pryce and J. G. Vos, *Coord. Chem. Rev.*, 256(2012) 2571−2600.
19. T. Abe, H. Imaya and M. Kaneko, *J. Porphyr. Phthalocya.*, 1(1997) 315-321.
20. G.F. Manbeck and E. Fujita, *J. Porphyr. Phthalocya.*, 19(2015) 1-20.
21. N. Sonoyama, M. Kirii and T. Sakata, Electrochem. Commun., 1(1999) 213-216.
22. J. Shen, R. Koterlever and M.T.M. Koper, *Nature Commun.*, 6(2015) 8177-8184.
23. M.T. de Groot and M.T.M. Koper, *Phys. Chem. Chem. Phys.*, 10(2008) 1023-1031.
24. A.H. Wonders, T.H. Housmans and M.T.M. Koper, *J. Appl. Electrochem.*, 36(2006) 1215-1221.
25. Y. Kwon and M.T.M. Koper, *Anal.Chem.*, 82 (2010) 5420-5424.
26. S. Yamazaki, Y. Yamada and K. Yasuda, *Inorg. Chem. Commun.*, 43(2004) 7263-7265.
27. 27． K. Miyamoto and R. Asahi, *J. Phys. Chem. C*, 123(2019) 9944-9948.
28. M. Abdinejad, C. Dao, B. Deng, F. Dinic, O. Voznyy, X Zhang and H.B. Kraatz, *ACS Sustain. Chem. & Eng.*, 8(2020) 9549-9557.
29. C. Costenin, M. Robert and J-M Savéant, *Science*, 338(2012) 90-94.
30. T. Cheng, H. Xiao and W.A. Goddard, *J. Am. Chem. Soc.*, 138(2016) 13802-13805.
31. Y. Z. Zhou, S. H. Chen, S. B. Xi, Z. T. Wang, P. L. Deng, F. Yang, Y. J. Han, Y. J. Pang, and B. Y. Xia, *Cell Rep. Phys. Sci.*, 1(2020) 100182-100194.
32. A. Lashgari, C.K. Williams, J. Glover, Y. Wu, J.C Chai and J.B. Jiang, *Chem. Eur. J.*, 26(2020) 16774-16781.
33. J. Choi, J. Kim, P. Wagner, S. Gambhir, R. Jailili, S. Byun, S. Sayyar, Y.M. Lee, D.R. Macfarlane, G.G. Wallace and D.L. Officer, *Energy Environ. Sci.*, 12(2019) 747-755.
34. Y.Y. Birdja, J. Shen and M.T.M. Koper, *Catal. Today*, 288(2017) 37-47.
35. A.J. Göttle and M.T.M. Koper, *J. Am. Chem. Soc.*, 140(2018) 4826-4834.
36. C. Römelt, J. Song, M. Tarrago, J.A. Rees, M. van Gastel, T. Weyhermüller, S. DeBeer, E. Bill, F. Neese and S. Ye, *Inorg. Chem.*, 56(2017) 4745-4750.
37. A.J. Göttle and M.T.M. Koper, *Chem. Sci.*, 8(2017) 458-465.
38. J. Shen, M. Kolb and M.T.M. Koper, *J. Phys. Chem. C*, 120(2016) 15714-15721.
39. V. Grass, D. Lexa, M. Momenteau and J.M. Saveant, *J. Am. Chem. Soc.*, 119(1997), 3536-3542.